Bulletin of Electrical Engineering and Informatics
Vol. 4, No. 1, March 2015, pp. 32~42
ISSN: 2089-3191

H-GA-PSO Method for Tuning of a PID Controller for a Buck-Boost Converter Modeled with a New Method of Signal Flow Graph Technique

Leila Mohammadian[1], Ebrahim Babaei*[2], Mohammad Bagher Bannae Sharifian[3]
Faculty of Electrical and Computer Engineering, University of Tabriz, Tabriz, Iran
*Corresponding author, e-mail: le.mohammadian@tabrizu.ac.ir[1], e-babaei@tabrizu.ac.ir[2], sharifian@tabrizu.ac.ir[3]

Abstract

In this paper, a new method of signal flow graph technique and Mason's gain formula are applied for extracting the model and transfer functions from control to output and from input to output of a buck-boost converter. In order to investigate necessity of a controller for the converter with assumed parameters, the frequency and time domain analysis is done and the open loop system characteristics are verified. In addition, the needed closed loop controlled system specifications are determined. Moreover, designing a controller for the mentioned converter system based on the extracted model is discussed. For this purpose, a proportional-integral-derivative (PID) controller is designed and the hybrid of genetic algorithm (GA) and particle swarm optimization (PSO), called H-GA-PSO method is used for tuning of the PID controller. Finally, the simulation results are used to show the performance of the proposed modeling and regulation methods.

Keywords*: Buck-boost converter, genetic algorithm, particle swarm optimization, model based controller, PID controller, signal flow graph*

1. Introduction

Recently, the dc-dc converters such as buck-boost converters are widely used in industrial applications. To design an effective controller for a dc-dc converter, a good and proper model of the converter is needed [1-2]. In order to get frequency response of the converters to design a controller and compensator circuits, the modeling of the system is inevitable. The model describes how control actions and disturbances are expected to affect the behavior of the system [3-4]. Previous works present different models for dc-dc converters. Considering that the power electronic converters include nonlinear elements like switches and diodes, then modeling of them needs linearization. So, applying averaging and linearization techniques has a special importance. After linearization, the inside model of the system is extractable and therefore investigating the frequency response will be possible [5-6].

Modeling the dc-dc converters by using small signal linearization and averaging techniques causes complexity in equations. Solving these equations for basic converters is not a problem, but for high order converters, dealing with them will be more difficult.

In [7], authors present both nonlinear and average linear models for a dc-dc converter. In [8-9], in order to derive a mathematical model of a dc-dc converter and study the transient states of it, a combination of Laplace and Z-transforms is employed.

Although a converter including switches is a nonlinear system, but it can be decomposed to two linear circuits; one for on-state and the other for off-state of the switch. Then, these two linear circuits are illustrated by means of two signal flow graphs. Composition of the two sub-graphs using switching branches reaches to the graph of the whole converter. Switching branches are the only nonlinear parts of the converters. Thus modeling process is limited to the switching branches. In [10-15] a signal flow graph method is proposed for modeling a dc-dc converter, then using Mason's gain formula any desired transfer function of the system might be extracted and used to design any proper controller.

This paper focuses on modeling of this converter by means of a new method of signal flow graph technique. Then by analyzing the obtained models, the performance of the converter is investigated. The proposed technique here, gives greatly simplified mathematical and

Received October 29, 2014; Revised November 27, 2014; Accepted December 16, 2014

graphical representation of the systems based on signal flow graph of the converter. The methods pose great advantage because of simplicity and being capable of giving any desired transfer function of the system to design a controller for a determined variable. Furthermore, by using the proposed graphical method, the intended models can be extracted and used for surveying nonlinear and dynamic behavior of switching converters.

Many control strategies have been presented to obtain the desired output voltage in dc-dc converters. In past, the controller design was based on using small signal linearization. Linear PID and PI controllers of the converters are usually designed by using standard frequency response techniques based on small signal model of the converter by using linear control theories such as Ziegler-Nichol's method, root locus technique, hysteresis method, Bode plot and etc [16-20]. Although these control methods based on the linearized small signal model of the converter have good performance around the operating point, but the small signal model changes with variations of the operating point. The poles and a right-half-plane zero, as well as the magnitude of the frequency response, depend on the duty cycle. Therefore, it is difficult for the PID controller to treat well with the variations of the operating point and they show poor performance subjecting to large load variations. Many PID tuning methods have been introduced until now. The Ziegler-Nichols method is an experimental one that is widely used. One disadvantage of this technique is the necessity of the prior knowledge regarding the controlled system model. In addition, the transient response of the system will not be good enough if the system dynamic changes. Non-linear control techniques such as fuzzy logic approach and sliding mode control may give better static and dynamic response.

In this paper, a hybrid optimization technique is applied to design a PID controller for a buck-boost converter. The design of PID controller parameters is considered as an optimization task and the controller parameters are determined by using H-GA-PSO technique. In addition, an appropriate fitness function is derived for above objective and is used in the evolutionary optimization. The attributes of the signal flow graph model of the converter together with that of the hybrid evolutionary algorithm yield a robust PID controller which rejects the disturbances.

The main contribution of this paper is to derive the model of the converter using the presented signal flow graph method and then designing a model- based controller for the buck-boost converter. In this process, by applying the mentioned signal flow graph technique and Mason's gain formula, the input to output, control to output transfer functions are obtained. Then, the frequency domain responses in form of Bode magnitude and phase diagrams are achieved and the proper PID controller tuned with a hybrid evolutionary method [16] is designed. At last, the simulation results based on the presented modeling and controlling methods are brought to show the good performance and behavior of the modeling and control methods.

2. Review on Buck-Boost DC-DC Converter

The output voltage of a buck-boost dc-dc converter can be more or less than the input voltage. The converter has two operational modes. The first mode is when the switch is on and the second one is for off state of the switch. In both modes, the switch and the diode would be turned on complementary. The output voltage has the opposite polarity of the input voltage. So, the converter is also referred to as a reverser converter. Figure 1(a) shows the power circuit of the buck-boost dc-dc converter. In this figure, v_g is the input voltage, L, C, R and R_L refer to the inductor, capacitor, load resistor and parasitic resistance of the inductor, respectively. v_L and v_o are the inductor voltage and the output voltage, respectively. i_g, i_L and i_o are the input current, inductor current and the output current, respectively. The two mentioned operational modes of the converter are shown in Figures 1(b) and 1(c).

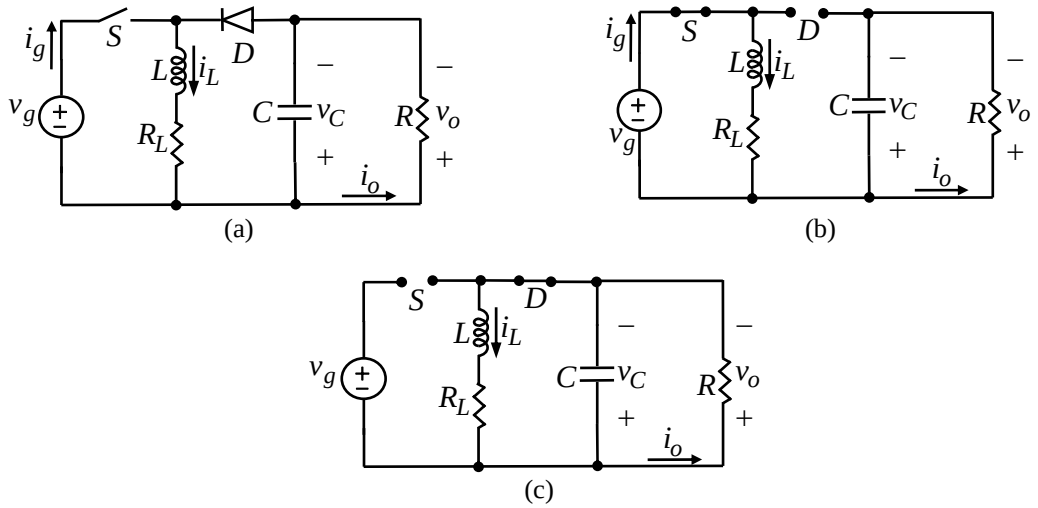

Figure 1. Buck-boost dc-dc converter; (a) power circuit; (b) equivalent circuit in on-state of switch; (c) equivalent circuit in off-state of switch

3. Proposed Graph Modeling Method

Before designing a controller for a system, the control system designer must know the system's characteristics. For example, is the open-loop system stable? Are there dominant poles? Are there poles that may be neglected during design? Is the system controllable by using the selected inputs? Can an estimator be designed based on the measured outputs? These types of questions should be answered before trying to design a controller for a system.

The nonlinear circuit of the converter is modeled as a small-signal continuous linear time invariant (LTI) system by using averaging technique. The model is a mathematical description of the behavior of the real system that is enough for performing stability test.

3.1. The Proposed Modeling Procedure

In order to model the converter by using the proposed method, the below steps should be done:

- First, the state equations for both operational modes are extracted by using kirchhoff's voltage and current laws.
- Then, the obtained state equations at the on time interval is multiplied in $\bar{d}_1$ and at the off time interval is multiplied in $1-\bar{d}_1=\bar{d}_2$, then they are added to each other. $\bar{d}_1$ is considered as the switch conduction coefficient and $\bar{d}_2$ as the switch non-conduction coefficient. The range of $\bar{d}_1$ is in 0 and 1 interval. The result is the averaged equations. Hence, the averaged equations are related to both on and off states of the switch. In averaged equations, the variables in form of $\bar{x}$ are average values which are different from the instantaneous variables in form of x.
- In averaged equations, dc and ac variables are substituted and rewritten with $\bar{X}$ and $\tilde{x}$, respectively. Considering all variables in form of $x=\bar{X}+\tilde{x}$ small signal linearization is done. Regarding that the product of two dc variables is a dc one and the product of one dc and one ac variable is an ac variable, also the product of two ac variables is zero, the obtained equations are rewritten.
- Finally, the extracted ac equations from the previous step are used to achieve the signal flow graph of the converter.

The state equations, the averaged and linearized form of them are given in Table 1.

The model of the converter without the parasitic resistor of the inductor is extracted by using the proposed graphical method.

Table 1. Achieved equations from converter operating in two modes, averaged and linearized form of them

State equations for Figure 1(b)	State equations for Figure 1(c)
$L\frac{di_L}{dt}=v_g$	$L\frac{di_L}{dt}=v_o$
$v_C=v_o$	$v_C=v_o$
$C\frac{dv_o}{dt}=-\frac{v_o}{R}$	$C\frac{dv_o}{dt}=-\frac{v_o}{R}+i_L$
The averaged equations for both modes	
$L\frac{d\bar{i}_L}{dt}=\bar{d}\bar{v}_g-(\bar{d}_2)\bar{v}_o$	
$C\frac{d\bar{v}_o}{dt}=-\frac{\bar{v}_o}{R}+(\bar{d}_2)\bar{i}_L$	
Small signal linearization on averaged equations	**The simplified equations after linearization**
$Ls(\tilde{i}_L+\bar{I}_L)=(\bar{D}_1+\tilde{d})(\tilde{v}_g+\bar{V}_g)-(\bar{D}_2-\tilde{d})(\tilde{v}_o+\bar{V}_o)$	$Ls\tilde{i}_L=\bar{D}_1\tilde{v}_g+\bar{V}_g\tilde{d}-(\bar{D}_2)\tilde{v}_o+\bar{V}_o\tilde{d}$
$Cs(\tilde{v}_o+\bar{V}_o)=-\frac{\tilde{v}_o}{R}-\frac{\bar{V}_o}{R}+(\bar{D}_2-\tilde{d})(\tilde{i}_L+\bar{I}_L)$	$Cs\tilde{v}_o=-\frac{\tilde{v}_o}{R}+(\bar{D}_2)\tilde{i}_L-\bar{I}_L\tilde{d}$
DC equations	**Small signal ac equations**
$\bar{V}_o=\frac{\bar{D}_1\bar{V}_g}{\bar{D}_2}$	$s\tilde{i}_L=\frac{\bar{D}_1}{L}\tilde{v}_g+\frac{\bar{V}_g}{L\bar{D}_2}\tilde{d}-\frac{\bar{D}_2}{L}\tilde{v}_o$
$\bar{I}_L=\frac{\bar{V}_o}{R\bar{D}_2}=\frac{\bar{D}_1\bar{V}_g}{R\bar{D}_2^{\,2}}$	$s\tilde{v}_o=-\frac{\tilde{v}_o}{RC}+\frac{\bar{D}_2}{C}\tilde{i}_L-\frac{\bar{D}_1\bar{V}_g}{RC\bar{D}_2^{\,2}}\tilde{d}$

3.2. Signal Flow Graph of the Converter

The ac small signal equations are used to plot the signal flow graph shown in Figure 2. In these equations, there are two variables; $\tilde{v}_o$ and $\tilde{i}_{L1}$, and two inputs; $\tilde{d}$ and $\tilde{v}_g$ .The graph is depicted for all independent variables $(s\tilde{x}, \tilde{x})$ by using nodes and paths between two nodes. In order to extract transfer functions from signal flow graph, Mason's gain formula $\left(\frac{y_{out}}{y_{in}}=\sum_{k=1}^{n}\frac{P_k\Delta_k}{\Delta}\right)$ will be used.

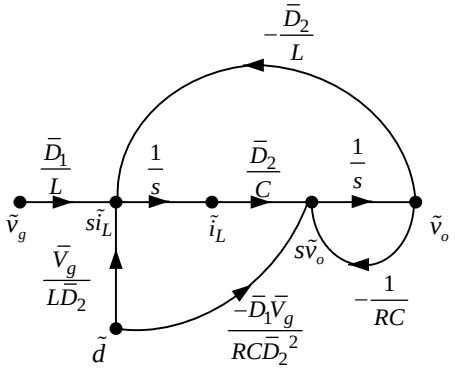

Figure 2. Signal flow graph for the buck-boost converter by using the proposed method

3.3. Signal Flow Graph of the Converter

To extract transfer functions, the gain of distinct loops, non-touching loops, forward paths from each input to output are calculated as Table 2. The obtained transfer functions in existence and absence of the parasitic resistance of the inductor are given in Table 3.

Table 2. Loop and path information of the signal flow graph and the obtained transfer functions

Distinct loops	**Distinct loops gain**	**Non-touching loops gain**
$Lp_1 : s\tilde{i}_L \to \tilde{i}_L \to s\tilde{v}_o \to \tilde{v}_o \to s\tilde{i}_L$ $Lp_1 : s\tilde{v}_o \to \tilde{v}_o \to s\tilde{v}_o$	$Lp_1 = -\frac{\bar{D}_2{}^2}{LCs^2}$ $Lp_2 = -\frac{1}{RCs}$	Does not exist.
Forward paths **Paths from $\tilde{v}_g$ to $\tilde{v}_o$**	**gain**	Δ_g
$P_g : \tilde{v}_g \to s\tilde{i}_L \to \tilde{i}_L \to s\tilde{v}_o \to \tilde{v}_o$	$P_g = \frac{\bar{D}_1\bar{D}_2}{LCs^2}$	$\Delta_g = 1$
Forward paths **Paths from $\tilde{d}$ to $\tilde{v}_o$**	**gain**	Δ_d
$P_{1d} : \tilde{d} \to s\tilde{i}_L \to \tilde{i}_L \to s\tilde{v}_o \to \tilde{v}_o$ $P_{2d} : \tilde{d} \to s\tilde{v}_o \to \tilde{v}_o$	$P_{1d} = \frac{\bar{V}_g}{LCs^2}$ $P_{2d} = -\frac{\bar{D}_1\bar{V}_g}{RC\bar{D}_2{}^2 s}$	$\Delta_{d1} = 1$ $\Delta_{d2} = 1$
Transfer function from $\tilde{v}_g$ to $\tilde{v}_o$		
$\frac{\tilde{v}_o}{\tilde{v}_g} = \sum \frac{P_g \Delta_g}{\Delta} = \frac{P_g}{1 - Lp_1 - Lp_2} = \frac{R\bar{D}_1\bar{D}_2}{RLCs^2 + Ls + R\bar{D}_2{}^2}$		
Transfer function from $\tilde{d}$ to $\tilde{v}_o$		
$\frac{\tilde{v}_o}{\tilde{d}} = \sum \frac{P_d \Delta_d}{\Delta} = \frac{P_{1d} + P_{2d}}{1 - Lp_1 - Lp_2} == \frac{\bar{V}_g (R - \frac{\bar{D}_1 L}{\bar{D}_2{}^2} s)}{RLCs^2 + Ls + R\bar{D}_2{}^2}$		

Table 3. The transfer functions for buck-boost converter in existence of the parasitic resistor of the inductor and without it

Transfer functions in existence of the parasitic resistor of the inductor (R_L)	**Transfer functions in absence of the parasitic resistor of the inductor (R_L)**
$\frac{\tilde{v}_o}{\tilde{v}_g} = \frac{\frac{D_1}{D_2}}{\left(\frac{LC}{D_2{}^2}\right)s^2 + \left(\frac{R_L C + \frac{L}{R}}{D_2{}^2}\right)s + \left(1 + \frac{(\frac{R_L}{R})}{D_2{}^2}\right)}$	$\frac{\tilde{v}_o}{\tilde{v}_g} = \frac{RD_1D_2}{RLCs^2 + Ls + RD_2{}^2}$
$\frac{\tilde{v}_o}{\tilde{d}} = \frac{V_g + V_o - \left(\frac{Ls + R_L}{D_2}\right)I_L}{D_2\left(\left(\frac{LC}{D_2{}^2}\right)s^2 + \left(\frac{R_L C + \frac{L}{R}}{D_2{}^2}\right)s + \left(1 + \frac{(\frac{R_L}{R})}{D_2{}^2}\right)\right)}$	$\frac{\tilde{v}_o}{\tilde{d}} = \frac{V_g\left(R - \frac{D_1 L}{D_2{}^2}s\right)}{RLCs^2 + Ls + RD_2{}^2}$

4. Proposed PID controller

In order to investigate the behavior of the converter from stability point of view, a buck-boost converter with the given parameters in Table 4 is considered.

Table 4. The buck-boost converter component values

L	$0.43\,mH$
C	$33\,\mu F$
R	10Ω
R_L	0.25Ω
V_g	$15V$

The root-locus diagrams for extracted transfer functions of the converter are shown in Figure 3. The information obtained from these diagrams is given in Table 5. For analysis purpose the duty cycle of the converter is supposed to be 0.335. Figure 4 shows the magnitude and phase Bode diagrams.

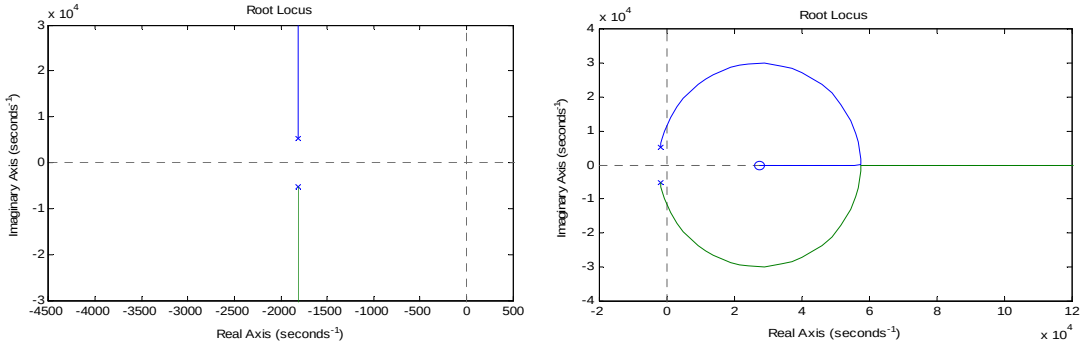

(a) (b)

Figure 3. Root locus diagram for (a) $\tilde{v}_o/\tilde{v}_g$; (b) $\tilde{v}_o/\tilde{d}$ with $R_L = 0.25\Omega$

Table 5. Information obtained from poles and zeros of the transfer functions of the model

	The transfer function $\tilde{v}_o/\tilde{v}_g$	The transfer function $\tilde{v}_o/\tilde{d}$	
	Poles	**Poles**	**Zero**
Value	$(-1.81 \pm 5.27i)\times 10^3$	$(-1.81 \pm 5.27i)\times 10^3$	2.77×10^4
Damping	0.324	0.324	-1
Overshoot (%)	34.1	34.1	0
Frequency (rad/s)	5.57×10^3	5.57×10^3	2.77×10^4

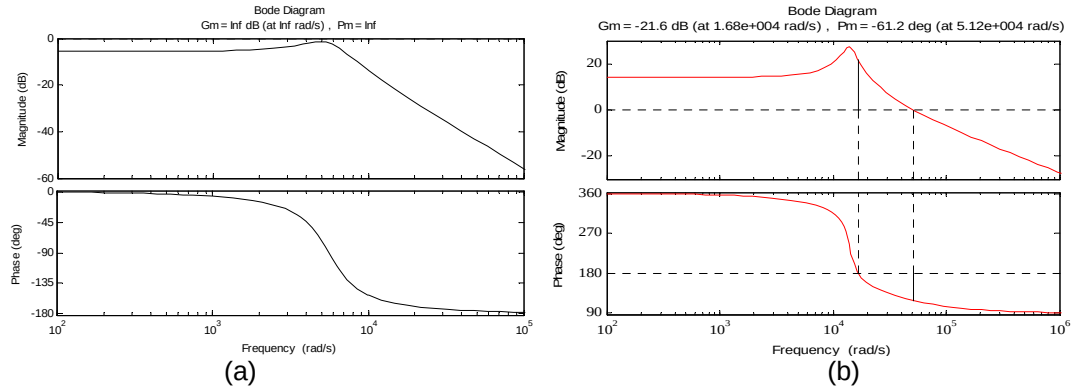

(a) (b)

Figure 4. Bode diagrams for (a) $\tilde{v}_o/\tilde{v}_g$; (b) $\tilde{v}_o/\tilde{d}$

From simulation results, it can be concluded that $\tilde{v}_o/\tilde{d}$ is unstable and phase and gain margins for $\tilde{v}_o/\tilde{d}$ are $GM = -21.6\,dB$ and $PM = -61.2\deg$, respectively. From root-locus diagrams, the mentioned system has a zero in right hand side of the imaginary margin. In order to have a more stable system the proper controller should be designed for the mentioned transfer function. At the following, a model-based PID controller by using H-GA-PSO tuning method will be explained.

The whole configuration of the controller beside the controlled system is plotted in Figure 5. In order to control the converter based on the previously extracted model, the PID controller is added to the controlled transfer function of the converter.

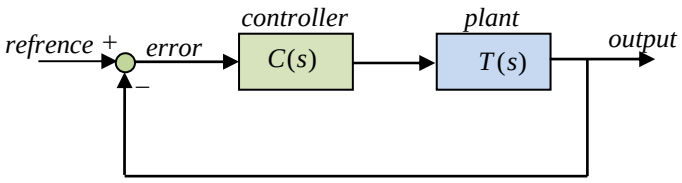

Figure 5. The whole system configuration with the PID controller

The PID controllers are widely used because they have only three parameters that has to be tuned for the process control. The input of a PID controller is an error signal which is the difference between the measured value and a desired reference signal for a process variable. The controller minimizes the error by tuning three constant parameters namely the proportional term (K_P), the integral term (K_I) and the differential term (K_D). Because of its simple configuration, the PID controller is the most commonly used control method in industry. The important aims of the PID controllers are:

- eliminating steady-state error of the step response (due to the integral action)
- reducing the peak overshoot (providing damping due to derivative action)

There are many methods for tuning the PID parameters or gains. The most famous method for achieving the mentioned goal is Ziegler-Nichols tuning method. Here, an evolutionary optimization technique called H-GA-PSO method is applied to get the desired PID parameters to get the desired stable system.

4.1. Proposed Computational Algorithm for Tuning the Parameters of the PID Controller

In GA, each individual represents a point in the search space and hence a possible solution to the problem. A population consists of a finite number of individuals. Each individual is decided by an evaluation mechanism to obtain its fitness value. Based on this fitness value and undergoing genetic operators, a new population is iteratively generated with each successive population referred to as a generation. The GA uses three basic operators (reproduction, crossover, and mutation) to manipulate the genetic composition of a population.

The PSO conducts searches by using a population of particles which correspond to the individuals in GA and randomly is generated. Each particle represents a potential solution and has a position represented by a position vector $(\bar{x}_i)$, A swarm of particles moves through the problem space with the moving velocity of $\bar{v}_i$. At each time step, a function (f_i) representing a quality measure is calculated using x_i as input. Each particle keeps track of its own best position, which is associated with the best fitness it has achieved so far in a vector v_i. Further, the best position among all the particles obtained so far in the population is kept track of as p_g. At each time step, by using the individual best position $(p_i(t))$ and global best position $(p_g(t))$ a new velocity for the particle is updated as follows:

$$\bar{v}_i(t+1) = \chi\{(\bar{v}_i(t) + C_1\phi_1[\bar{p}_i(t) - \bar{x}_i(t)] + C_2\phi_2[\bar{p}_g(t) - \bar{x}_i(t)]\} \quad (1)$$

where C_1 and C_2 are positive constants, ϕ_1 and ϕ_2 are uniformly distributed random numbers in [0,1] interval and χ controls the magnitude of v.

Changing velocity in this way enables the particle i to search around its individual best position (p_i) and global best position (p_g). Based on the updated velocities, each particle changes its position according to the following equation:

$$\overline{x}_i(t+1) = \overline{x}_i(t) + \overline{v}_i(t+1) \quad (2)$$

The computation of PSO is easy and adds only a slight computation load when it is incorporated into GA. The detailed design algorithm of H-GA-PSO consists of three major operators: enhancement, crossover and mutation. In H-GA-PSO, GA and PSO both work with the same population. Based on the encoding scheme, P_s individuals forming the population are randomly generated. These individuals may be regarded as chromosomes in terms of GA, or as particles in terms of PSO. Then, new individuals in the next generation are created by enhancement, crossover and mutation operations [21- 22]. For clarity, the flow of these operations is illustrated in Figure 6.

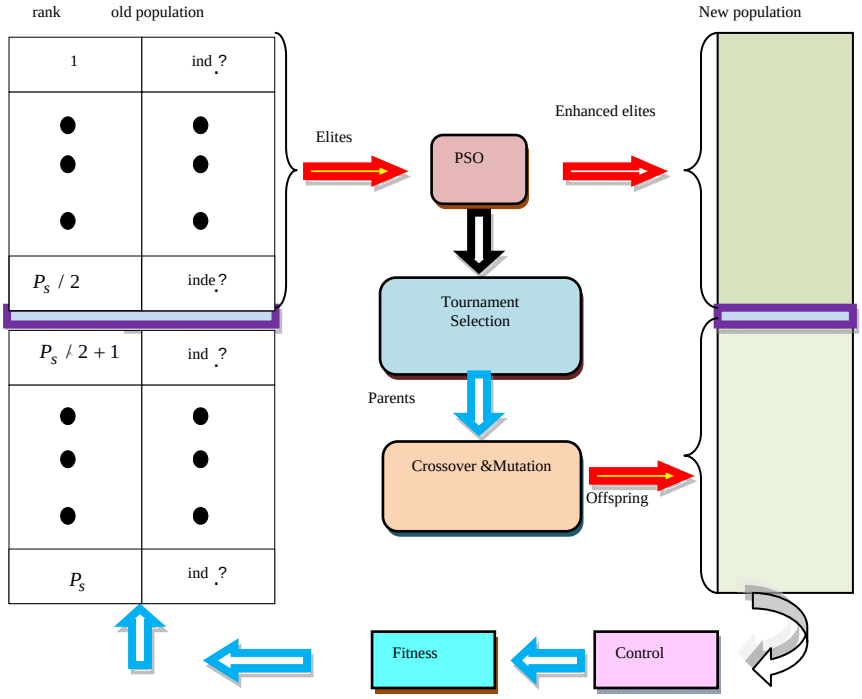

Figure 6: Flowchart of the H-GA-PSO method

Enhancement, crossover, and mutation operators are described as follows:

Enhancement: After the fitness in each generation with GA, the values of all the individuals in the same population are calculated and the top-half best-performing ones are marked. These individuals are regarded as elites. Instead of reproducing the elites directly to the next generation of GA, first the elites are enhanced by PSO. By using the enhanced elites as parents, the generated offspring will usually achieve better performance than those bred by original elites. The group constituted by the elites is regarded as a swarm, and each elite corresponds to a particle in it. By performing PSO on the elites, we may increase the search ability. Half of the population in the next generation is occupied by the enhanced individuals, others by crossover operation.

Crossover: To produce well performing individuals, in the crossover operation, parents are selected from the enhanced elites. To select parents for the crossover operation, the tournament-selection scheme is used in which two enhanced elites are selected at random, and their fitness values are compared to select the elite with better fitness value as one parent. Then the other parent is selected in the same way. Two offspring are created by performing crossover on the selected parents. Two-point crossover operation is used, where two crossover sites are randomly selected within the range of an individual and swapping occurs. These produced offspring occupy half of the population in the next generation.

Mutation: In H-GA-PSO, mutation occurs in conjunction with the crossover operation. Here, uniform mutation is adopted, that is, the mutated gene is randomly drawn, uniformly from the corresponding search interval. In the simulations, a constant mutation-probability $P_m = 0.1$ is used.

4.2. Computation and Problem Formulation of the Proposed H-GA-PSO Technique

Based on the proposed algorithm, the software was developed using Matlab for proper selection of PID gain to control the buck-boost converter.

The main target of this paper is improving the dynamic response of the buck-boost converter by using proper controller parameters. The following parameters are considered as the main objectives of optimization:

Rise Time (T_R), Settling Time (T_S), Overshoot $(O.S)$, Undershoot $(U.S)$ and Steady state error (E_{SS}). Regarding the mentioned parameters, the optimization problem is as below:

$$J = (1+T_R)*(1+T_S)*(1+O.S)*(1+U.S)*(1+E_{SS}) \quad (3)$$

Subject to constraints which keep the PID gains in a predetermined interval. Here the interval is considered in [0, 50].

5. Simulation Results

The optimization problem is solved by using H-GA-PSO technique and the optimization process and final fitness value is shown in Figure 7. The optimized fitness value is about 1.03823. The controller parameters after applying proposed H-GA-PSO technique and the used parameters for optimization are given in Table 6. Table 7 shows the stability information of the converter system before and after applying the proposed H-GA-PSO tuned PID controller.

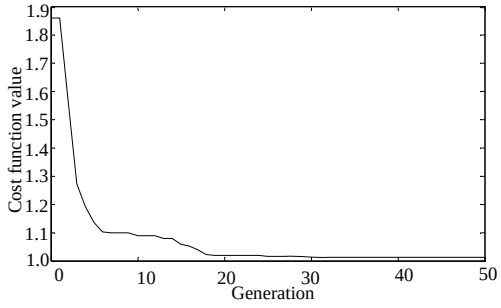

Figure 7. Fitness optimized by using proposed H-GA-PSO method

Table 6. PID parameters obtained from proposed H-GA-PSO method and the used parameters in optimization

K_P	0
K_I	31.36
K_D	0
Population size	50
Max iterations	20

Table 7. Stability information of the converter system obtained before and after applying the proposed H-GA-PSO tuned PID controller

Step response and frequency domain information	before applying the controller	after applying the controller
T_R(s)	6.5394×10^{-5}	0.0136
T_S(s)	0.0021	0.0243
O,S(%)	76.5176	0
U.S(%)	14.6460	0
E_{SS}	4	0
Phase Margin	-61.2 deg	89.4deg
Gain Margin	-21.6 *dB*	25.8*dB*
Closed loop stable?	No	Yes

Figure 8 shows the step response of the system before and after applying the designed PID controller. This shows that the open-loop system does not reject disturbances on the input voltage and cannot regulate the output voltage.

Figure 9 shows the Bode diagrams of the system after applying the designed PID controller. The results prove the stability of the obtained system with the proposed controller.

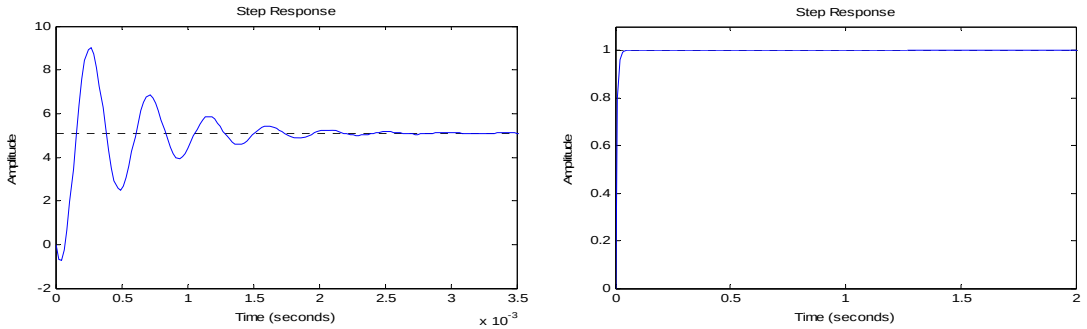

(a) (b)

Figure 8. Step response of the converter system; (a) without controller; (b) with proposed H-GA-PSO tuned PID controller

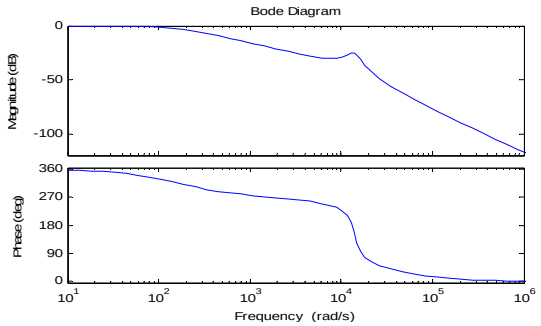

Figure 9. Bode diagrams of the converter system after applying proposed H-GA-PSO tuned PID controller

From the simulation results, it is obvious that the disturbance is rejected and this controller behaves very desirably in time-domain. Checking the bode diagrams depicts that the system has become a stable one. Also, calculations bring out the gain margin as $25.8dB$ and a phase margin of 89.4deg which are favorite frequency-domain response characteristics. Then, applying the proposed controller, the converter system becomes stable and regulated.

6. Conclusions

In this paper, the application of a new method of the signal flow graph technique and Mason's gain formula to extract the associated transfer functions and modeling a buck-boost converter is investigated. The transfer functions from input to output and control to output have been obtained. Employing the obtained functions, the stability analysis and deciding about the controller design is performed. Finally, the efficiency of the proposed H-GA-PSO tuned PID controller as a model based technique to design a proper control system is shown. The proposed control system employs the PID controller with a special adjustment for proper setting of the control responses.

References

[1] Wei X, Tsang KM, Chan WL. DC/DC buck converter using internal model control. *Journal of Electr. Power Compo. Sys.* 2009; 37(3): 320-330.
[2] Yalamanchili KP, Ferdowsi M, Lu Sh, Xiao P, Corzine K. Derivation of double-input dc-dc power electronic converters. *Journal of Electr. Power Compo. Sys*. 2011; 39(5): 478-490.
[3] Luo FL, Ye H. Small signal analysis of energy factor and mathematical modeling of power dc-dc converters. *IEEE Trans. Power Electron*. 2007; 22(1): 69-79.
[4] Priewasser R. Modeling, control and digital implementation of dc-dc converters under variable switching frequency operation. Ph.D. Thesis. 2012; Klagenfurt university.
[5] Kapat S. Control methods for improving the performance of dc-dc converters. Ph.D. Thesis. 2009; Kharagpur, India.
[6] Wong LK, Man TK. Small signal modeling of open-loop SEPIC converters. *IET Power Electron*. 2010; 3(6): 858-868.
[7] Mashinchi Mahery H, Babaei E. Mathematical modeling of buck–boost dc–dc converter and investigation of converter elements on transient and steady state responses. *Electr. Power and Ener. Sys.* 2013; 44: 949-963.
[8] Babaei E, Mashinchi Maheri H. Analytical solution for steady and transient states of buck dc–dc converter in CCM. *Arab. Journal Sci. and Eng.* 2013; 38(12): 3383-3397.
[9] Veerachary M. General rules for signal flow graph modeling and analysis of dc-dc converters. *IEEE Trans. Aerospace Electron. Sys.* 2004; 40(1): 259–271.
[10] Veerachary M. Signal flow graph modeling of multi-state boost dc–dc converters. *IEE -Electr. Power Appl*. 2004; 151(5): 583-589.
[11] Veerachary M. Analysis of fourth-order dc-dc converters: A flow graph approach. *IEEE Trans. Ind. Electron*. 2008; 55(1): 133-141.
[12] Veerachary M, Senjyu T, Uezato K. *Signal flow graph nonlinear modeling analysis of IDB converter*. in Proc. ISIE, Korea, 2001: 1066-1070.
[13] Stefani RT, Shahian B, Savant CJ, Hostetter GH. Design of feedback control systems. 4th ed. New York, NY: *Oxford University Press*, 2002.
[14] Zhu M, Luo FL. Super-lift dc-dc converters: graphical analysis and modeling. *Journal Power Electron*. 2009; 9(6): 854-865.
[15] Luo FL, Ye H. Advanced dc/dc converters. *CRC Press*, London.
[16] Kamri D, Larbes Ch. Observer-based control for dc–dc converters. *Arab. Journal Sci. and Eng.* 2014; 39(5): 4089-4102.
[17] Ogata K. Modern Control Engineering. *Prentice-Hall of India Press*, New Delhi.
[18] Salimi M, Soltani J, Markadeh GhA, Abjadi NR. Adaptive nonlinear control of the dc-dc buck converters operating in CCM and DCM. *Int. Trans. Electr. Energy Sys*. 2013; 23(8): 1536–1547.
[19] Tsang KM, Chan WL. Non-linear cascade control of dc-dc buck converter. *Journal of Electr Power Compo. and Sys*. 2008; 36(9): 977-989.
[20] Renaudineau H, Martin J, Mobarakeh BN, Pierfederici S. DC-DC converters dynamic modeling with state observer-based parameter estimation. *IEEE Trans. Power Electron*. 2014; 99(1): 1-9.
[21] Mohammadian L, Khani S, Mohammadian A, Tarafdar Hagh M, Babaei E. Using a hybrid evolutionary method for optimal planning, and reducing loss of distribution networks. *Intl. Res. J. Appl. Basic. Sci.* 2012; 3: 2734-2744.
[22] Feng LCh, Feng JCh. Evolutionary fuzzy control of flexible AC transmission system. *IEE Proc.-Gener. Transm. Distrib*. 2005; 152(4): 441-448.